Journal of the European Ceramic Society 15 (1995) 1065–1070

0955-2219(95)00094-1
0955-2219/95/$9.50

Influence of 1 vol% Ni_3Al Addition on Sintering and Mechanical Properties of Reaction-Bonded Si_3N_4.

B. R. Zhang[a]* & F. Marino[b]

[a]Department of Inorganic Materials, Shandong Institute of Light Industry, 250100 Jinan, People's Republic of China
[b]Dipartimento di Scienza dei Materiali e Ingegneria Chimica, Politecnico di Torino, 10129 Torino, Italy

(Received 5 December 1994; revised version received 24 May 1995; accepted 25 May 1995)

Abstract

The sintering-aid effect of 1 vol% Ni_3Al powder addition on the nitridation of silicon at 1300–1350°C for 5–20 h and its influence on mechanical properties of the reaction sintered material have been studied. The addition of 1 vol% Ni_3Al accelerates the nitriding rate of silicon and promotes the formation of β-Si_3N_4; no free silicon phase was detected by X-ray diffraction in the 1 vol% Ni_3Al-added sample nitrided at 1350°C for 20 h. The 1 vol% Ni_3Al-added sintered material has higher relative density, higher Vickers hardness and indentation fracture toughness but lower Young's modulus and flexural strength than the contemporaneously processed reaction-bonded silicon nitride.

1 Introduction

Reaction-bonded silicon nitride (RBSN) is formed by reacting a silicon powder preform with either nitrogen or ammonia. Its outstanding characteristic is that net shape components can be prepared because no shrinkage occurs during the process, which leads to the formation of complex shapes without the expensive machining associated with sintering and hot-pressing processes. Another important advantage of reaction bonding is the absence of oxide sintering aids which degrade the high-temperature mechanical properties of sintered and hot-pressed materials.[1] In addition, combination of the advantages of the reaction-bonding process (lower shrinkage rate during sintering and lower raw material costs, compared with Si_3N_4 powder compacts) with those of hot isostatic pressing (HIP) (high density and excellent mechanical properties) has been considered,[2–4] using RBSN as starting material for HIP or sintering. The post-sintering and post-HIP of RBSN have resolved the high porosity (12–30 vol%) problem of RBSN.[5]

RBSN formation from conventional powders typically requires several days at temperature ranging up to 1420°C,[5] resulting in mainly α-Si_3N_4 phase. Our previous studies[6,7] on reaction-bonded sintering of Si_3N_4 intermetallic composite have demonstrated that the addition of Ni_3Al powder accelerates the nitridation of silicon and promotes the formation of β-Si_3N_4 phase at a low temperature such as 1250°C through the presence of some liquid phase resulting from the reaction between Ni_3Al and Si, accompanied by the formation of intermetallic compounds of the type Ni_xSi_y. Accordingly, the anomalous thermal hardening nature of Ni_3Al, i.e. the strength increases with temperature,[8] cannot be utilized. On the other hand, when the amount of Ni_3Al addition was small, e.g. 1 vol%, the nitriding rate of silicon and the resulting relative density of the Si + 1 vol% Ni_3Al sample were higher than that of the contemporaneously processed silicon compact without Ni_3Al;[7] but it was also found that there was still free silicon phase being detected in the Si + 1 vol% Ni_3Al sample nitrided at 1250°C for up to 80 h. Therefore, in this paper, a new nitriding process of the Si + 1 vol% Ni_3Al system is investigated, in which Ni_3Al is used as a sintering aid. The resulting micro-structure as well as the influence of the Ni_3Al addition on mechanical properties are reported.

2 Experimental Procedure

Commercial silicon powders were ball-milled to a particle size of < 1 μm and mixed with 1 vol% of rapidly solidified Ni_3Al particles (about 20 μm) with respect to the final Si_3N_4. These intermetallic powders, produced by vacuum gas atomization and with the composition 73·12 Ni–18·82 Al–8·06 Cr–0·019 Mo–0·10 B at% (kindly supplied by

*Present address: Dipartimento di Scienza dei Materiali e Ingegneria Chimica, Politecnico di Torino, 10129 Torino, Italy.

R. N. Wright and J. R. Knibloe[9]), have a ductile behaviour. The powder mixtures were cold-pressed using a single-action stainless steel die and formation pressure of 250 MPa, producing green compacts with a density of about 62% of the theoretical value. The reaction sintering was carried out at 1300–1350°C for 5–20 h; the nitriding gas was a mixture of purified N_2+5% H_2, at atmospheric pressure. Pure silicon compacts were nitrided under the same conditions as reference material. The samples without Ni_3Al and with 1 vol% Ni_3Al are named SN and SN/NA1, respectively. The extent of nitridation was determined by the ratio between the weight of the nitrided sample (minus the weight of Ni_3Al added) and its theoretical weight assuming that all the silicon is converted into Si_3N_4.

The nitrided phases were identified by X-ray diffraction (XRD), using Cu$K\alpha$ radiation monochromated in the diffracted beam, on the core of samples; the α/β ratio was determined by the quantitative X-ray analysis method outlined by Gazzara and Messier.[10] Microstructure was characterized by scanning electron microscopy (SEM) on polished surfaces and on samples etched using a 10% HF+15% HNO_3 solution for 14 h. Densities of samples were determined before and after nitriding by weight and volume measurements and by Archimedes' principle. Bending strength of rectangular bars (3 mm × 4 mm × 45 mm) was measured at room temperature by four-point bending using spans of 40 and 20 mm at a crosshead speed of 1 mm min^{-1}. The Vickers microhardness was measured using loads from 9·8 to 196 N. The elastic modulus was measured by dynamic mechanical analysis (DMA) at room temperature. Fracture toughness was determined by the indentation crack length technique, calculated using the formula of Anstis *et al;*[11] the induced crack length and its propagation were observed by optical microscopy and SEM. Both the fracture toughness and the hardness were measured using five indentations for each specimen.

3 Results and Discussion

3.1 Effect of Ni_3Al addition on nitridation of Si and resulting microstructure

The reaction-sintering processes applied and the resulting nitrided fraction are shown in Table 1, which indicates that the nitrided fraction of the SN/NA1 sample is much higher than that of SN sintered in the same process. These values are consistent with the results reported in our previous work,[7] which concluded that the acceleration effect of Ni_3Al addition on the nitriding rate of Si was mainly due to the presence of some liquid phase resulting from the reaction between Si and Ni_3Al, leading to the formation of low melting intermetallics of the type Ni_xSi_y. The nitrided fraction of Si in SN/NA1 has been determined by the ratio between the weight of the nitrided sample and its theoretical weight minus the weight of Ni_3Al added (both at numerator and denominator), assuming that all the silicon in the sample is completely nitrided, as listed in Table 1. It is also supposed that the weight of Ni_3Al remains the same before and after sintering.

Higher temperatures and shorter times (1300–1350°C; 5–20 h) are employed in the present study and higher nitriding rates obtained, compared with the processes (1250°C; 5–80 h) and the nitrided fraction reported in our previous work.[7] Typically, no free silicon phase is detected in SN/NA1 nitrided at 1350°C for 20 h; the X-ray diffraction patterns of SN/NA1 and, for comparison, SN nitrided under the same condition are shown in Fig. 1. The α/β ratio in reaction-sintered SN/NA1 is about 6/4. In addition, no Ni_3Al but some nickel silicides have been detected which melt at about 1000°C and are considered to be responsible for the formation of β-modification Si_3N_4. In this work, it was difficult to identify the formulae of the nickel silicides accurately, because their amount is very small. For the SN sample, the nitrided fraction increases with increasing temperature and, as shown in Fig. 1, a small amount of β-Si_3N_4 has been found in SN nitrided at 1350°C for 20 h.

As the reaction between silicon and nitrogen is exothermic, it may result in overheating of the sample and this phenomenon would be more important when the nitriding temperature applied is sufficiently high. On the other hand, the presence of a small amount of metallic impurities can also decrease the melting temperature of silicon and accelerate the formation of β-Si_3N_4.[12,13] However, a large amount of free silicon has been also detected

Table 1. Nitrided fraction of the samples obtained under different sintering processes

Sample	*Nitrided fraction (%) under following processes*			
	1300°C, 5 h	*1300°C, 15 h*	*1300°C, 5 h+ 1350°C, 5 h*	*1350°C, 20 h*
SN	77·2	79·2	82·0	89·1
SN/NA1	85·3	89·2	91·3	95·2

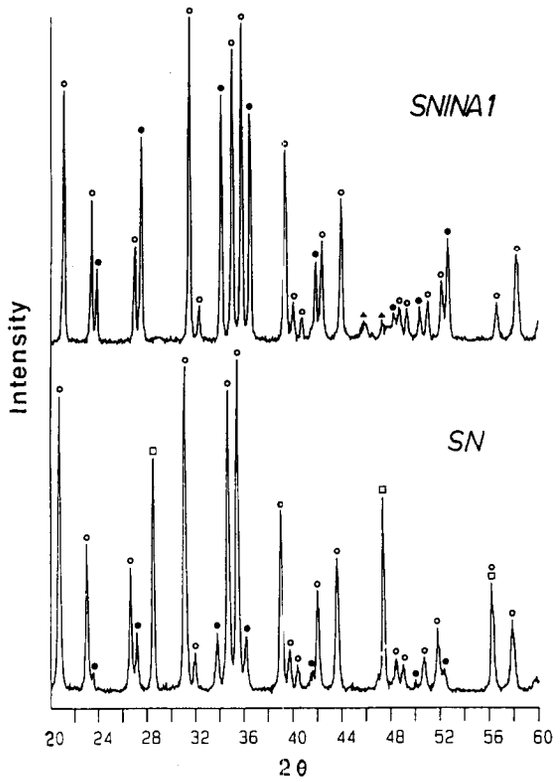

Fig. 1. X-ray diffraction patterns of the samples nitrided at 1350°C for 20 h: (○) α-Si_3N_4, (●) β-Si_3N_4, (□) Si, (▲) Ni_xSi_y.

by X-ray diffraction on the inner region of a cross-sectioned sample. This indicates that the surface is nitrided more rapidly than the bulk region for the pure silicon compact. On the contrary, no difference was found by X-ray diffraction analyses on the surface or the inner part of the SN/NA1 nitrided compact.

Figure 2 shows the morphology of SN/NA1 sintered at 1350°C for 20 h. The light particles are intermetallics, mainly nickel silicides, whose formulae have been determined on the sample containing 10 vol% Ni_3Al[6] and chiefly correspond to NiSi, $Ni_{31}Si_{12}$, Cr_3Si. It must be emphasized

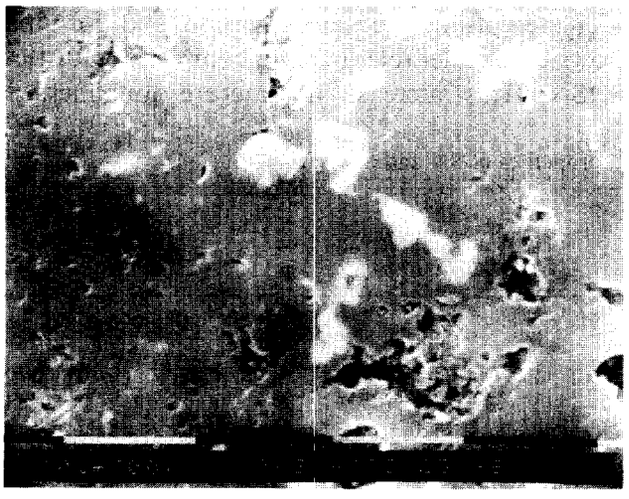

Fig. 2. SEM micrograph showing the morphology of SN/NA1 sample nitrided at 1350°C for 20 h.

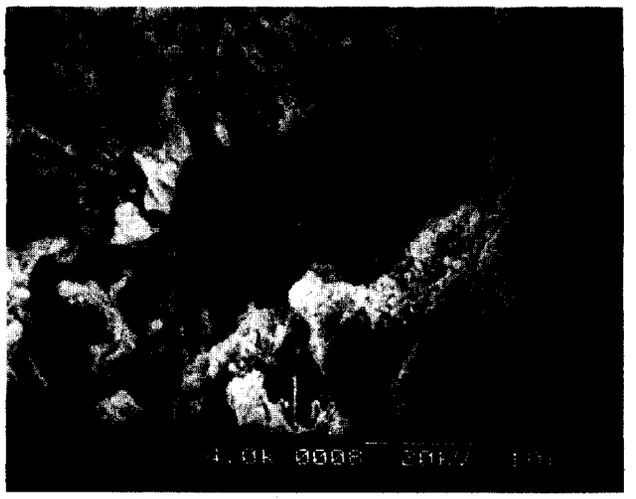

Fig. 3. SEM micrograph of an etched SN/NA1 sample, showing the cavity left by an intermetallic particle.

that more macropores (1–3 μm) were found in SN/NA1, probably owing to the reaction between Si and Ni_3Al, and this results in a less homogeneous microstructure than in SN. As indicated by X-ray diffraction analyses in Fig. 1, the microstructure of SN/NA1 consists of α-Si_3N_4, β-Si_3N_4 and traces of Ni_xSi_y intermetallics. SEM observation reveals that α-phase present in SN/NA1 contains α-grains and α-whiskers; α-grains are generally formed in zones far from intermetallic particles. On the contrary, α-whiskers and β-modification Si_3N_4 are preferably generated close to macropores and intermetallic particles because of the occurrence of some liquid phase. This is consistant with the formation mechanism of α-whisker and β-modification Si_3N_4 indicated in the literature.[5,14] Figure 3 shows a SEM micrograph of an etched SN/NA1 sample; in the cavity left by an intermetallic particle, α-whiskers and the rod-like β-Si_3N_4 are observed, as shown more clearly in Fig. 4 for α-whiskers and Fig. 5 for β-phase.

Fig. 4. SEM micrograph showing α-whiskers formed in macropores.

Fig. 5. SEM micrograph showing β-Si_3N_4 formation in zone close to an intermetallic particle.

3.2 Influence of Ni_3Al addition on densification and mechanical properties of the composite

Table 2 shows the densities and mechanical properties of the SN/NA1 sample compared with two different samples of RBSN: one nitrided under the same conditions (1350°C, 20 h), the other having about the same nitrided fraction.[7]

The relative densities of SN and SN/NA1 nitrided at 1350°C for 20 h are about 80 and 90%, respectively, obtained from the ratio of the measured density and $3{\cdot}16 \times 10^3$ kg m^{-3} for SN and $3{\cdot}20 \times 10^3$ kg m^{-3} (calculated) for SN/NA1. SN/NA1 is denser than SN obtained under the same nitriding process due to the higher conversion rate of the silicon and the $\alpha \rightarrow \beta$ phase transformation of Si_3N_4,[15] although it has a less homogeneous microstructure than SN.

It should be mentioned that the values of flexural strength are not reported in Table 2 because of high scattering of the experimental data, which however show a decreasing trend of the flexural strength from SN to SN/NA1. Thus, for the mechanical properties, it can be said that the addition of 1 vol% Ni_3Al increases the Vickers hardness and the fracture toughness, but decreases the Young's modulus and the flexural strength, compared with both RBSN samples. The hardness of SN/NA1 was expected to decrease because both the Ni_3Al and Ni_xSi_y intermetallic phases are softer than silicon nitride, but the experimental results have shown a little increase, probably owing to the improvement of the relative density. As regards the decrease of the flexural strength of SN/NA1, a very significant influencing factor is the microstructure, especially the pore size. As indicated by Ziegler *et al.*[5] a homogeneous microstructure with a narrow pore-size distribution at moderate densities is better than a high-density material which contains large voids in order to achieve high-strength materials. Furthermore, the decrease in strength caused by large pores, formed during reaction bonding of the coarse-grained silicon powder, was demonstrated in the same paper. Thus, the presence of more macropores in the SN/NA1 sample results in the decrease in strength; on the other hand, it may be also responsible for the decrease of Young's modulus in SN/NA1. Even though a study on hot-pressed Si_3N_4[16] has illustrated an increase of strength with increasing amount of β-fraction and although a large amount of β-grains was found in SN/NA1, no improvement of strength was observed for this sample, perhaps owing to the inhomogeneous distribution of β-phase.

However, in contrast to reduced flexural strength, the indentation fracture toughness of SN/NA1 is higher than that of SN. Although it must be kept in mind that many formulae for the determination of K_{IC} from indentation are proposed in the literature,[17] each of them leading to different indentation toughness values,[18] the indentation crack length technique is still widely applied for toughness measurement of Si_3N_4 ceramics.[18,19] In the present work, the values of indentation fracture toughness for SN, ranging from 1·99 to 2·20 Mpa $m^{1/2}$, fall in the typical range of K_{IC} values, 1·5–2·8 MPa $m^{1/2}$, for RBSN.[5] The K_{IC} value of SN/NA1, calculated using the same method and formula, shows a considerable increase compared with that of SN. This increase in fracture toughness is

Table 2. Relative densities and mechanical properties of SN and SN/NA1

Property	*SN (1350°C, 20 h)*	*SN*[7] *(1250°C, 50 h + 1450°C, 10 h)*	*SN/NA1 (1350°C, 20 h)*
Nitrided fraction (%)	89·1	94·9	95·2
Relative density (%)	79·75	85·44	89·80
Vickers microhardness (GPa)	7·86	8·10	8·35
Young's modulus, E (RT, GPa)	110	120	100
Fracture toughness, K_{IC}(MPa a $m^{1/2}$)	1·99	2·20	2·54

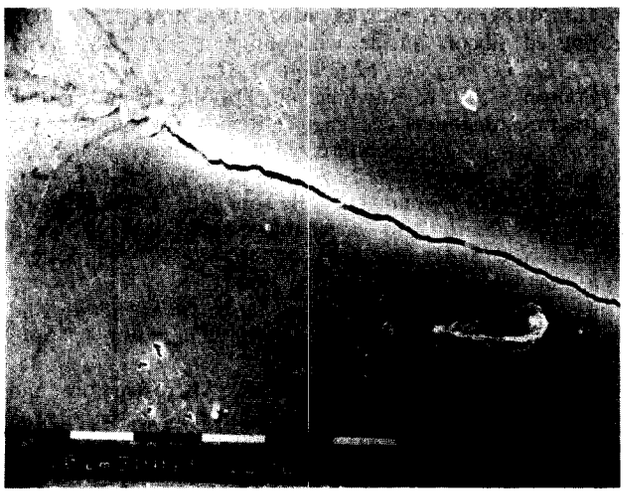

Fig. 6. SEM micrograph showing the crack propagation in SN sample.

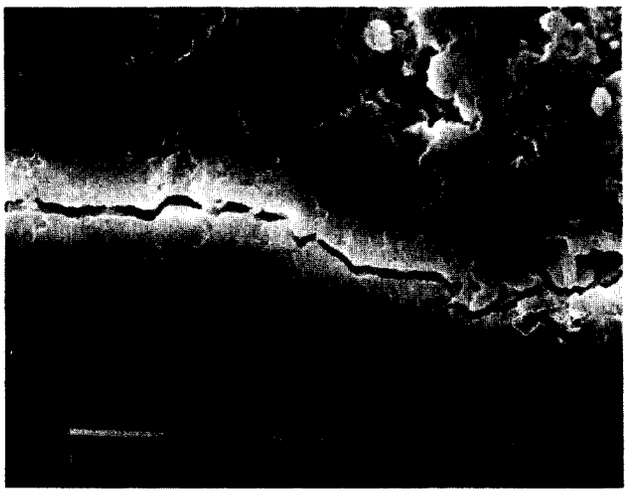

Fig. 7. SEM micrograph showing the crack propagation in SN/NA1 sample.

probably due to the formation of rod-like β-Si_3N_4 phase in SN/NA1 which, as reported in the literature,[19–22] shows the self-reinforcement and crack-bridging effects of the *in situ* formed β-Si_3N_4. Figures 6 and 7 show the propagation of the crack induced by the indentation in SN and SN/NA1, respectively, using a load of 196 N. It can be observed that the crack propagates smoothly in the SN sample and that it has an indented path, which causes energy consumption, around the weak intermetallic/matrix interface in SN/NA1.

4 Conclusions

The reaction-sintering processes of Si+1 vol% Ni_3Al at 1300–1350°C in purified N_2+5% H_2 atmosphere have been investigated. The addition of 1 vol% Ni_3Al accelerates the nitriding rate of silicon and increases the relative density of the resulting nitrided samples. No free silicon phase is detected by XRD in 1 vol% Ni_3Al-added samples nitrided at 1350°C for 20 h. The resulting nitrided fraction and the relative density are 95·2% and 89·80%, respectively, compared with 89·1% and 79·75% for the contemporaneously processed RBSN. The microstructure of SN/NA1 consists of α, β-Si_3N_4 with an α/β ratio of about 6/4, and a small amount of nickel silicide intermetallics; but SN/NA1 has more macropores than SN.

The Vickers hardness and the indentation fracture toughness of SN/NA1 are respectively 8·35 GPa and 2·54 MPa $m^{1/2}$, higher than those of SN owing to the higher relative density and the formation of rod-like β-modification Si_3N_4; but the Young's modulus and the flexural strength are slightly lower than in SN probably due to the presence of more macropores in SN/NA1.

Acknowledgements

This work was partially supported by Alenia Spazio spa Torino (Italy) and the authors gratefully acknowledge the collaboration of Dr B. Fornari, Alenia Spazio spa Torino. We would like also to thank Professor O. Sbaizero, Università di Trieste (Italy) for his help in the four point-bending tests, Dr M. Ferraris and M. Raimondo, Dipartimento di Scienza dei Materiali e Ingegneria Chimica del Politecnico di Torino, for their help with the SEM observations.

References

1. Sheldon, B. W., Szekely, J. & Haggerty, J. S., Formation of reaction-bonded silicon nitride from silane-derived silicon powders: macroscopic kinetics and related transport phenomena. *J. Am. Ceram. Soc.*, **75** (1992) 677–85.
2. Kleebe, H. J. & Ziegler, G., Influence of crystalline secondary phases on the densification behaviour of reaction-bonded silicon nitride during postsintering under increased nitrogen pressure. *J. Am. Ceram. Soc.*, **72** (1989) 2314–17.
3. Heinrich, J., Backer, E. & Bohmer, M., Hot isostatic pressing of Si_3N_4 powder compacts and reaction-bonded Si_3N_4. *J. Am. Ceram. Soc.*, **71** (1988) C28–9.
4. Mangels, J. A. & Tennenhouse, G. J., Densification of reaction-bonded silicon nitride. *Am. Ceram. Soc., Bull.*, **59** (1980) 1216–22.
5. Ziegler, G., Heinrich, J. & Wotting, G., Relationships between processing, microstructure and properties of dense and reaction-bonded silicon nitride. *J. Mater. Sci.*, **22** (1987) 3041–86.
6. Zhang, B. R., Gialanella, S. & Marino, F., Chemical aspects of reaction-bonded sintering of Si_3N_4 intermetallic composite. In *Proc. of the 8th CIMTEC. Int. Conf. on Modern Materials Technologies.* Techna, Faenza, Italy, 1994,
7. Marino, F., Zhang, B. R. & Fornari, B., Processing and microstructural development of reaction-bonded sintering of a Si_3N_4 intermetallic composite. *J. Mater. Sci.*, submitted.

8. Guard, R. W. & Westbrook, J. H., Alloying behaviour of Ni_3Al. *Trans. TMS-AIME*, **215** (1959) 807.
9. Wright, R. N. & Knibloe, J. R., The influence of alloying on the microstructure and mechanical properties of P/M Ni_3Al. *Acta Metall. Mater.*, **38** (1990) 1993–2001.
10. Gazzara, C. P. & Messier, D. R., Determination of phase content of Si_3N_4 by X-ray diffraction analysis. *Am. Ceram. Soc. Bull.*, **56** (1977) 777-80.
11. Anstis, G. R., Chanticul, P., Lawn, B. R. & Marshall, D. B., A critical evaluation of indentation techniques for measuring fracture toughness: I, Direct crack measurements. *J. Am. Ceram. Soc.*, **64** (1981) 533–8.
12. Mitomo, M., Effect of Fe and Al additions on nitridation of silicon. *J. Mater. Sci.*, **12** (1977) 273–276.
13. Messier, D. R., Riley, F. L. & Brook, R. J., The α/β silicon nitride phase transformation. *J. Mater. Sci.*, **13** (1978) 1199–1205.
14. Messier, D. R. & Wong, P., Kinetics of nitridation of Si powder compacts. *J. Am. Cream. Soc.*, **56** (1973) 480–5.
15. Mitomo, M. & Mizuno, K., Sintering behaviour of Si_3N_4 with Y_2O_3 and Al_2O_3 addition. *Yogyo Kyokaishi*, **94** (1986) 106–11.
16. Himsolt, G. & Knoch, H., Mechanical properties of hot-pressed silicon nitride with different grain structures. *J. Am. Ceram. Soc.*, **62** (1979) 29–32.
17. Ponton, C. B. & Rawlings, R. D., Vickers indentation fracture toughness test Part 1: Review of literature and formulation of standardized indentation toughness equations. *Mater. Sci. Technol.*, **5** (1989) 865–72.
18. Rossignol, F., Goursat, P., Besson, J. L. & Lespade, P., Microstructure and mechanical behaviour of self-reinforced Si_3N_4 and Si_3N_4 – SiC whisker composites. *J. Eur. Ceram. Soc.*, **13** (1994) 299–312.
19. Travitzky, N. A. & Claussen, N., Microstructure and properties of metal infiltrated RBSN composites. *J. Eur. Ceram. Soc.*, **9** (1992) 61–5.
20. Pyzik, A. J. & Beaman, D. R., Microstructure and properties of self-reinforced silicon nitride. *J. Am. Ceram. Soc.*, **76** (1993) 2737–44.
21. Becher, P. F., Microstructural design of toughened ceramics. *J. Am. Ceram. Soc.*, **74** (1991) 255–69.
22. Mitomo, M. & Uenosono, S., Microstructural development during gas-pressure sintering of α-silicon nitride. *J. Am. Ceram. Soc.*, **75** (1992) 103–8.